CHARACTERIZATION OF MOLD FILLING IN VACUUM INFUSION PROCESS

Young Seok Song

Centre for Composite Materials, University of Delaware Newark, DE 19716
Tel.: +1 (302) 831-2765, Fax:+1 (302) 831-8525, E-mail address: youngseoks@gmail.com

(Received ; accepted)

ABSTRACT

A study on mold filling in vacuum infusion process was carried out analytically. Three different compaction models were used to describe compaction behaviour of preforms. New analytic solutions were proposed for fibre volume fraction and pressure distributions, and an effective permeability was defined based on the solutions. In this study, the closed form equations introduced by Lopatnikov et al. [1] were modified to consider the preform compaction behaviour more exactly and the results of the modified equations were employed in an effort to verify the proposed analytic model. It was found that the very different pressure and fibre volume fraction profiles were developed during the resin infusion depending on the compaction behaviour of the preforms.

Keywords: mathematical characterization, vacuum infusion process.

1. INTRODUCTION

Vacuum infusion process (VIP) has been showing great potentials in many areas such as automobile, aerospace, marine, and construction industries [2-4]. Both the use of vacuum and the flexibility of a vacuum bag result in many advantages, which include low tooling cost, processability for complex and large parts, and reduction of labour. However, in contrast to a typical resin transfer molding (RTM) process, thickness of fibre preforms used in VIP changes depending on a resin flow pressure because they are not fully confined by a rigid mold [5,6]. Fig. 1 schematically illustrates the thickness variation during resin infusion in VIP. For analysis of the rein infusion, many numerical models have been reported and experimental works were carried out [7-9]. However, there is a lack of analytic studies on the resin infusion, which are capable of giving better understanding of the entire process. Lopatnikov et al. [1] and Hsiao et al. [10] proposed the closed form solutions of describing resin flow behaviour through fibrous porous media.

This study presents a new analytic model for VIP considering the compressibility of preforms, which are described by three different compaction models. The equations proposed by Lopatnikov et al. [1] were modified and compared with the analytic results. The main goal of this study is to investigate how the compaction behaviour of preforms affects thickness and pressure distributions in the resin-saturated preform.

2. THEORETICAL ANALYSIS

2.1. Modified equations

An infinitesimal strain for fibre preforms can be defined as:

$$\varepsilon = \frac{h - h_0}{h_0} \tag{1}$$

where h_0 is the original thickness of the preform. Lopatnikov et al. [1] assumed that the preform was purely elastic and suggested the following relation:

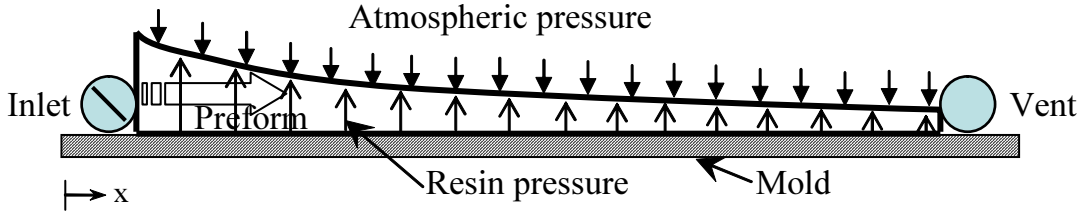


Fig. 1. Schematic illustration of vacuum infusion process.

$$P = E\varepsilon \tag{2}$$

here P and E denote the resin pressure and an elastic modulus for the preform, respectively. To model nonlinearity of the compaction behaviour more effectively, the following compaction model is proposed in this study.

$$P = \alpha(\varphi_0 + \varepsilon)^{\beta} - \alpha\varphi_0^{\beta} \tag{3}$$

where φ_0 is the original porosity of the preform. The parameter values used in this study are listed in Table 1. More detailed explanation was described in the literature [1]. Assuming that the preform material is incompressible, the following equation is obtained.

$$v_f h = v_0 h_0 \tag{4}$$

Following mathematical procedures similar to [1], the analytic solutions for resin flow through the preform can be obtained:

$$L(t) = \frac{\sqrt{2(\beta+4)t}}{\beta+3}\sqrt{\frac{k\alpha\beta}{\mu(1-\varphi_0)}}\frac{(\varphi_0+\varepsilon_0)^{\beta+3}-\varphi_0^{\beta+3}}{\sqrt{(\varphi_0+\varepsilon_0)^{\beta+4}-\varphi_0^{\beta+4}}} \tag{5}$$

$$h(x,t) = h_0 \left[\left\{-\frac{x}{\sqrt{2t}}\sqrt{\frac{\mu(1-\varphi_0)^2}{k\alpha\beta(\beta+4)}\left((\varphi_0+\varepsilon_0)^{\beta+4}-\varphi_0^{\beta+4}\right)}+(\varphi_0+\varepsilon_0)^{\beta+3}\right\}^{\frac{1}{\beta+3}} + 1 - \varphi_0\right] \tag{6}$$

$$P(x,t) = \alpha \left\{-\frac{x}{\sqrt{2t}}\sqrt{\frac{\mu(1-\varphi_0)^2}{k\alpha\beta(\beta+4)}\left((\varphi_0+\varepsilon_0)^{\beta+4}-\varphi_0^{\beta+4}\right)}+(\varphi_0+\varepsilon_0)^{\beta+3}\right\}^{\frac{\beta}{\beta+3}} - \alpha\varphi_0^{\beta} \tag{7}$$

2.2. Proposed equations

Combination of mass and momentum balances between resin and preforms yields the following unified model [4,11].

$$-\frac{1}{v_f}\frac{\partial v_f}{\partial t} - \frac{1}{v_f}\frac{\partial v_f}{\partial x}V_f = \frac{\partial}{\partial x}\left(\frac{K}{\mu}\frac{\partial P}{\partial x}\right) \tag{8}$$

where v_f is the fibre volume fraction, V_f is the velocity of fibres, and K is the permeability of fibre preforms. Assuming $V_f = 0$ due to a slow in-plane flow in VIP, equation (8) is simplified as:

$$-\frac{1}{v_f}\frac{\partial v_f}{\partial t} = \frac{\partial}{\partial x}\left(\frac{K}{\mu}\frac{\partial P}{\partial x}\right) \tag{9}$$

To consider a change in permeability with respect to the fibre volume fraction, the Kozeny-Carman model is adopted.

$$K = k\frac{(1-v_f)^3}{v_f^2} \tag{10}$$

where k is the Kozeny constant. Because the fibre volume fraction over the entire mold is not constant, the following power law equation is used to correlate the compaction pressure of the preforms with the fibre volume fraction.

$$v_f = aP_{comp}^{b} \tag{11}$$

where a and b mean the fibre volume fraction at 1 Pa and the stiffening index standing for the compressibility of the preform, respectively.

$$P_{comp} + P = P_{atm} \tag{12}$$

where P_{comp} is the compaction pressure, P denotes the resin flow pressure, and P_{atm} is the atmospheric pressure, 1 atm. Substituting equations (10)-(12) into equation (9) leads to:

$$\frac{1}{v_f}\frac{\partial v_f}{\partial t} = \frac{k}{ab\mu}\frac{\partial}{\partial x}\left(\frac{(1-v_f)^3}{v_f^2}v_f^{1/b-1}\frac{\partial v_f}{\partial x}\right) \tag{13}$$

Assuming a quasi-steady state for the flow, which can be justified by a characteristic time to reach the equilibrium distribution of deformations [1], equation (13) becomes:

$$\frac{\partial}{\partial x}\left(\frac{(1-v_f)^3}{v_f^2}v_f^{1/b-1}\frac{\partial v_f}{\partial x}\right) = 0 \tag{14}$$

Taking the integration of equation (14) over the flow advancement distance provides.

$$v_f^{1/b}\left(3b + \frac{b}{(1-2b)v_f^2} - \frac{3b}{(1-b)v_f} - \frac{bv_f}{1+b}\right) = A(t)x + B(t) \tag{15}$$

A and B are determined from the boundary conditions: $v_f = v_{f_0} = v_{\min}$ at $x = 0$ and $v_f = v_{\max}$ at $x = \mathrm{L}$.

To numerically obtain a flow front advancement with respect to time, the following mass conservation principle is applied over the preform saturated by resin.

$$\int_0^{L(t)} (1 - v_f) h dx = \int_0^t (1 - v_{f_0}) h(0,t) V(0,t) dt \tag{16}$$

where the resin velocity, *V(x,t)*, is a function of the elapsed time and the position. Using equation (4), equation (10) is rewritten as:

$$\frac{v_{f_0}}{1 - v_{f_0}} \int_0^L \frac{1 - v_f}{v_f} dx = \int_0^t V(0,t) dt \tag{17}$$

From equation (9), the following equations are obtained:

$$\frac{\partial v_f}{\partial x} = \frac{A(t) v_f^{3-1/b}}{(1 - v_f)^3} \tag{18}$$

The combination of Darcy's law with equations (10) and (11) can be expressed as follows:

$$V(x,t) = -\frac{K}{\mu} \frac{\partial P}{\partial x} = \frac{k}{\mu a b} (1 - v_f)^3 v_f^{1/b-3} \frac{\partial v_f}{\partial x} \tag{19}$$

Equations (18) and (19) give the resin velocity at the injection gate as below:

$$V(0,t) = \frac{k}{\mu a b} A(t) \Big|_{x=0} \tag{20}$$

After substituting equation (20) into equation (17) and applying the boundary condition at $x=L$, equation (17) is recast as:

$$A(t) L(t) + B(t) = C \tag{21}$$

Assuming a quasi-steady state, equation (17) becomes:

$$\frac{v_{f_0}}{1 - v_{f_0}} \frac{\mu a b}{k(C - B)} \int_0^L \frac{1 - v_f}{v_f} dx = \frac{t}{L(t)} \tag{22}$$

Changing the integration variable from the flow distance to the fibre volume fraction yields:

$$\frac{v_{f_0}}{1 - v_{f_0}} \frac{\mu a b}{k(C - B)^2} \int_{v_{\min}}^{v_{\max}} (1 - v_f)^4 v_f^{1/b-4} dv_f = \frac{t}{L(t)^2} \tag{23}$$

The analytic solution for the flow front advancement is written as the following:

$$\frac{v_{f_0}}{1 - v_{f_0}} \frac{\mu a b}{k(C - B)^2} \left[v_f^{1/b} \left(-4b + \frac{b}{(1 - 3b) v_f^3} + \frac{4b}{(2b - 1) v_f^2} + \frac{6b}{(1 - b) v_f} + \frac{b v_f}{1 + b} \right) \right]_{v_{\min}}^{v_{\max}} = \frac{t}{L(t)^2} \tag{24}$$

The flow front progression can be expressed in terms of the effective permeability as follows:

$$L^2 = \frac{K_{eff}}{\mu} t \tag{25}$$

The effective permeability is defined as:

$$\frac{1}{K_{eff}} = \frac{v_{f_0}}{1 - v_{f_0}} \frac{a b}{k(C - B)^2} \left[v_f^{1/b} \left(-4b + \frac{b}{(1 - 3b) v_f^3} + \frac{4b}{(2b - 1) v_f^2} + \frac{6b}{(1 - b) v_f} + \frac{b v_f}{1 + b} \right) \right]_{v_{\min}}^{v_{\max}} \tag{26}$$

Table 1: Parameters for compaction and flow models.

E (Pa)	2.0×10^5
α (Pa)	1.2×10^7
β	0.01
ε_0	0.45
φ_0	0.4
a	0.1
b	0.15
k (m^2)	1.0×10^{-9}
μ (Pa·s)	0.4

3. RESULTS AND DISCUSSION

The assumptions behind the analytic model proposed in this study are as follows: (i) the liquid resin is regarded as the Newtonian, laminar, and incompressible fluid, (ii) the flow-induced void formation and the air entrapment caused by the difference of capillary pressure and wettability are not dealt with [12], and (iii) the influence of distribution media on the flow front advancement is not considered.

Fig. 2 shows the comparison of the models used to describe the compaction behaviour of preforms. It is a well-known fact that a power law given as equation (11) is capable of fitting experimental compaction results very well [13]. Equation (3) modified in this study shows the different compaction behaviour from the linear model, but not enough compared to the power law. Fig. 3 presents the fibre volume fraction profiles with respect to the dimensionless distance, which is normalized by the flow front advancement distance. It is observed that the most concave fibre volume fraction distribution is obtained when the linear compaction model is utilized. Fig. 3 demonstrates that the totally different fibre volume fraction profiles are obtained depending on the compaction behaviour of the preforms. As the b value increases, the fibre volume fraction has a lower gradient near by the injection line of resin.

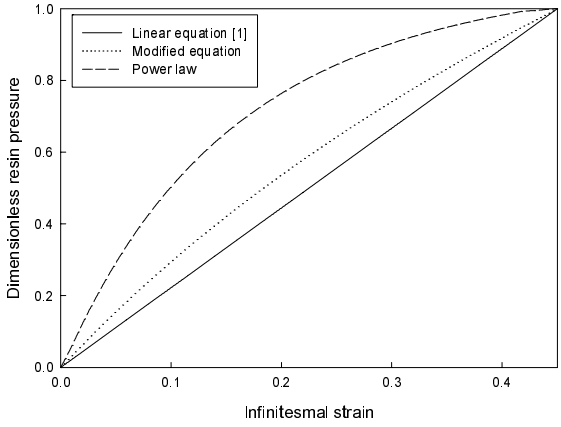


Fig. 2: Comparison of the compaction models used in this study.

Fig. 4 shows the dimensionless pressure fields across the entire mold. Unlike Fig. 3, more complex pressure ones are found. Increasing the b value leads to more curved pressure fields. It is found from equation (15) that the fibre volume fraction and the resin pressure fields are dependent on the only compaction behaviour of the preform but not permeability. The flow front advancement obtained by using the proposed model is displayed in Fig. 5. As the b value increases, the velocity of the flow front is raised. This is explained by the fact that higher b results in lower fibre volume fraction as shown in Fig. 4, which facilitates the flow front advancement.

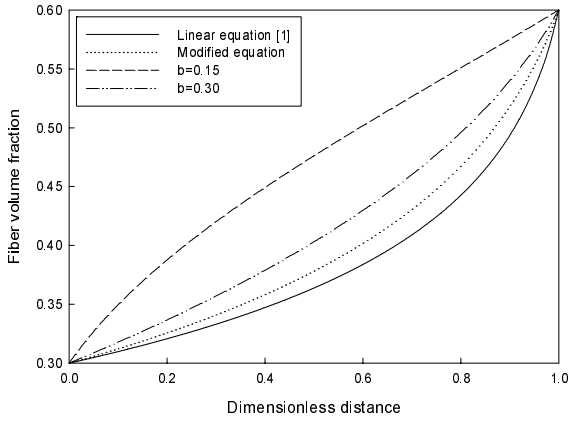


Fig. 3: Fibre volume fraction distributions as a function of distance.

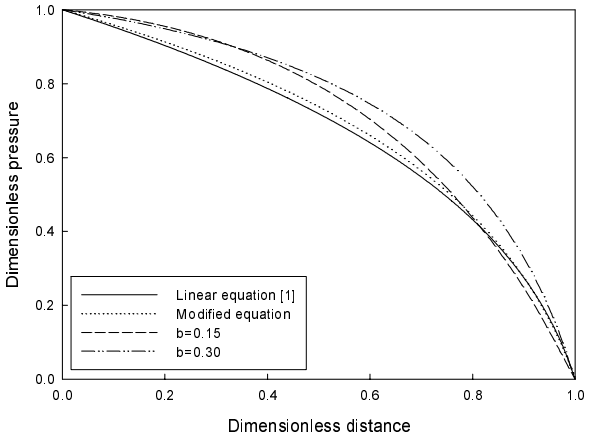


Fig.4: Resin pressure profiles during resin infusion with respect to dimentionless distance.

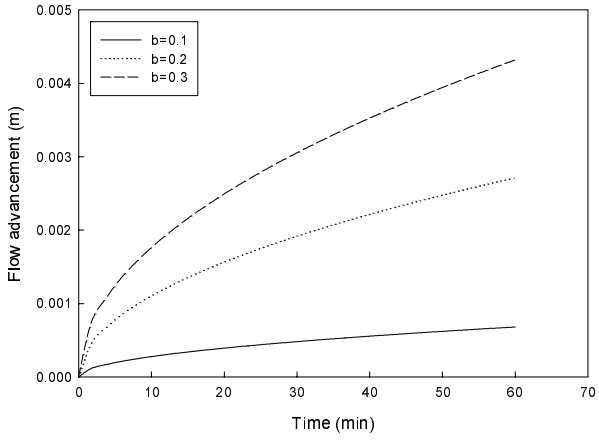


Fig.5: Flow front advancements as a function of time.

References:

1. **Lopatnikov, S., Simacek, P., Gillespie, Jr J.W. and Advani, S.G.,** 'A closed form solution to describe infusion of resin under vacuum in deformable fibrous porous media', *Modelling Simul Mater Sci Eng* **12** (2004), 191-204.
2. **Li, W., Krehl, J., Gillespie, J.R. Jr, Heider, D., Endrulat, M., Hochrein, K., Dunham, M.G. and Dubois, C.J.,** 'Process and performance evaluation of the vacuum-assisted process', *J Compos Mater* **38** (2004), 1803-1814.
3. **Tung, V.X. and Dhir, V.K.,** 'Finite element solution of multi-dimensional two-phase flow through porous media with arbitrary heating conditions', *Int J Multiphase Flow* **16** (1990), 985-1002.
4. **Kang, M.K., Lee, W.I. and Hahn, H.T.,** 'Analysis of vacuum bag resin transfer molding process', *Compos Part A* **32** (2001), 1553-1560.
5. **Andersson, H.M., Lundstrφm, T.S., Gebart, B.R. and Synnergren, P.,** 'Application of digital speckle photography to measure thickness variations in the vacuum infusion process', *Polym Compos* **24** (2003), 448-455.
6. **Walsh, S.M. and Freese C.E.,** 'Numerical model of relaxation during vacuum-assisted resin transfer molding (VARTM)', *Polym Compos* **26** (2005), 628-635.
7. **Johnson, R.J. and Pitchumani, R.,** 'Enhancement of flow in VARTM using localized induction heating', *Compos Sci Technol* **63** (2003), 2201-2215.
8. **Han, K., Jiang, S., Zhang, C. and Wang, B.,** 'Flow modeling and simulation of SCRIMP for composites manufacturing', *Comos Part A* **31** (2000), 79-86.
9. **Acheson, J.A., Simacek, P. and Advani, S.G.,** 'The implications of fibre compaction and saturation on fully coupled VARTM simulation', *Compos Part A* **35** (2004), 159-169.
10. **Hsiao, K.T., Mathur, R., Advani, S.G., Gillespie, Jr J.W. and Fink, B.K.,** 'A closed form solution for flow during the vacuum assisted resin transfer molding process', *J Manuf Sci Eng* **122** (2000), 463-475.
11. **Dave, R.,** 'A unified approach to modeling resin flow during composite processing', J Comp Mater **24** (1990), 22-41.
12. **Patel, N. and Lee, L.J.,** 'Modeling of void formation and removal in liquid composite molding. Part I: wettability anaysis', *Polym Compos* **17** (1996), 96-103.
13. **Robitaille, F. and Gauvin, R.,** 'Compaction of textile reinforcements for composites manufacturing. I: review of experimental results', *Polym Compos* **19** (1998), 543-557.